

Modeling of Particle Radiation Interaction in Solid Fuel Combustion with Artificial Neural Networks

Tim Gronarz*, Martin Habermehl, Reinhold Kneer

*Institute of Heat and Mass Transfer, RWTH Aachen University
Augustinerbach 6, 52056 Aachen*

Abstract

In the present investigation, artificial neural networks are applied to model scattering and absorption properties occurring in particle radiation interaction for numerical simulation of pulverized coal combustion. To determine averaged scattering and absorption properties, an averaging procedure over spectral incident radiation profile and particle size distribution is applied. These averaged properties then are approximated by means of an artificial neural network. A study to determine a suitable network architecture is performed.

Keywords: Scattering; absorption; Mie theory; artificial neural networks; function approximation

1. Introduction

For a reliable numerical simulation of solid fuel combustion processes, several physical effects have to be modeled accurately. This includes simulation of turbulent flow with particle tracking, pyrolysis of the particles and combustion of char and volatiles. Among these, scattering and absorption of thermal radiation by fuel and ash particles should be considered as well.

The interaction of particles and thermal radiation is determined by a variety of parameters: spectral distribution of incident radiation, size distribution and radiative properties of the particles. Since the particles are involved in a combustion process, their radiative properties and size distribution are changed as the burnout progresses. As a simplification, the particles are assumed to be spherical. To describe the variation of scattering and absorption properties, Mie theory for coated particles is applied in the present work. Averaging over a particle size distribution and the incident radiation profile in the infrared spectral range is performed. Thereby, spectral variations of the index of refraction are taken into account.

In a numerical solution of the radiative transport equation, a direct computation of the phase function and scattering and absorption efficiencies from Mie theory in each iteration step is not possible due to high computational demands. Thus,

adequate substituting strategies and/or models have to be applied.

Two steps in the process of determining the radiative properties can be described by a model. The first step is to model or store the amount of radiation, scattered into a discrete solid angle. Therefore, integration of the phase function over this solid angle has to be performed. This approach lacks flexibility, since the scattered intensity has to be stored for each angular discretization pattern that could potentially be applied in the simulation. The second approach aims at storing the value of the phase function at specific angles directly. A model applied at this stage needs to enable fast data access, a low memory requirement is required. Also, flexibility compared to applying the previously calculated data must be ensured. As soon as a discretization pattern is chosen, integration of the phase function has to be performed. In the present paper, a model for the second approach is presented.

Due to the complex dependency of scattering and absorption on the influential parameters, classical approximations such as linear or polynomial approaches are not well suited for modelling purposes. In order to capture the relevant characteristics, artificial neural networks are applied in this study.

Artificial neural networks (ANN) have been used in various applications in many diverse areas [1]. They are often used for function approximation, which simply means the mapping of an input to an output. However, one of their major advantages is the ability to produce reasonable outputs for inputs not encountered in training (interpolation). If the input val-

*Corresponding author

Email address: gronarz@wsa.rwth-aachen.de (Tim Gronarz)

ues are out of range of the training data, the network is able to extrapolate. However, extrapolation involves large uncertainties. Ihme et al. [2] applied artificial neural networks to represent chemistry in LES-Simulations of turbulent flames. They found an optimal architecture for all relevant thermochemical species. According to Ihme, a major advantage of neural networks in combustion simulations is their considerably lower storage requirement compared to tabulation approaches. Ihme et al. [2] also found that the retrieval of data from the network takes up to five times longer than retrieving data stored with a tabulation technique. Nevertheless, the time required for this retrieval is still low, compared to the overall computation time in LES Simulations. In general, they found good agreement between the results computed with an artificial network and a tabulation technique.

Aiming at the advantages mentioned before, artificial neural networks are applied in this study to model particle radiation interaction. First, suitable network architectures are identified followed by assessments of the approximation accuracy, the robustness and the training effort of the network.

2. Methods

2.1. Mie theory for coated particles

Mie theory [3, 4] yields a mathematical description of scattering and absorption of thermal radiation by spherical particles based on a solution of the Maxwell equations. This solution consists of a series of spherical harmonics with corresponding coefficients, called scattering coefficients. The calculation of the scattering coefficients as well as the evaluation of the spherical harmonics is computationally expensive.

In the present investigation, scattering and absorption properties are calculated depending on the burnout progress B of the particle. Therefore, Mie Theory for coated particles is applied [5, 6]. The inner core is assumed to consist of coal, surrounded by an outer layer consisting of ash. Each material is represented by the corresponding index of refraction.

2.2. Averaging of scattering and absorption properties

The averaged scattering phase function Φ is obtained by integrating over the infrared wavelength interval from $0.3 \mu\text{m}$ up to $12 \mu\text{m}$ and particle sizes from $D_{\min} = 0.8 \mu\text{m}$ to $D_{\max} = 200 \mu\text{m}$

$$\bar{\Phi} = \frac{1}{\bar{C}} \sum_{D_{\min}}^{D_{\max}} \left[\sum_{\lambda_{\min}}^{\lambda_{\max}} \Phi(x) Q_{sca}(x) E_{\Delta\lambda} \right] C(D) P_{\Delta D} \quad (1)$$

with the finite scattering angle interval $\Delta\theta$. ΔD and $\Delta\lambda$ denote that the distribution functions are integrated over the corresponding particle size or wavelength interval. A similar procedure is performed for scattering and absorption efficiencies Q_i :

$$\bar{Q}_i = \frac{1}{\bar{C}} \sum_{D_{\min}}^{D_{\max}} \left[\sum_{\lambda_{\min}}^{\lambda_{\max}} Q_i(x) E_{\Delta\lambda} \right] C(D) P_{\Delta D} \quad (2)$$

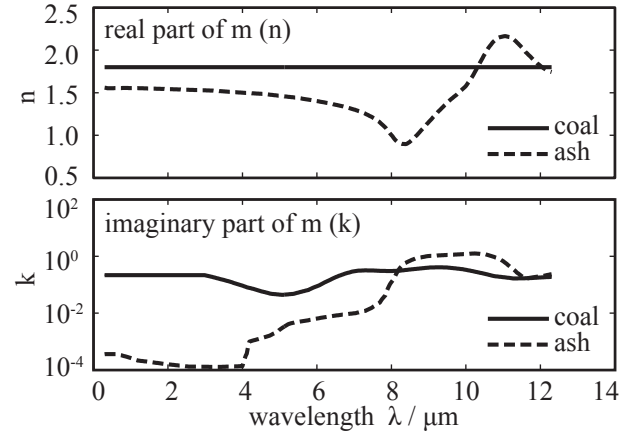


Figure 1: Indices of refraction as applied for coal and ash

with i denoting either sca or abs. x is the dimensionless size parameter and C is the cross section of the particle with diameter D . Weighting is performed with a Rosin-Rammler particle size distribution P , defined by an average diameter of D_m and a spread parameter of n_{RR} . The averaged cross section is calculated as $\bar{C} = \sum_{D_{\min}}^{D_{\max}} C(D) P_{\Delta D}$. Φ and Q depend on the complex refractive index m as well. m has been dropped from the equations to improve readability. Details on the averaging procedure can also be found in [7].

2.3. Index of Refraction, Particle size distribution and Burnout Progress

For the spectrally varying index of refraction of coal, data determined by Manickavasagam and Mengüç [8] were applied. Ash was modeled with the refractive index given by Neubronner [9]. The real and complex parts for the refractive indices are shown in Fig. 1. A Rosin-Rammler particle size distribution (PSD) was applied with mean diameters of $D_{m,coal} = 100 \mu\text{m}$, $D_{m,ash} = 10 \mu\text{m}$ and a spread parameter of $n_{RR} = 3.5$ for both cases. The variation of the mean diameter with burnout B is described by the following relationship:

$$D_m(B) = (D_c - D_a)(1 - B)^a + D_a \quad (3)$$

The inner diameter was calculated from the outer diameter by relating the volume of the outer layer to the volume of the entire particle

$$D_{\text{inner}} = \sqrt[3]{(1 - B)D_m} \quad (4)$$

In the present study, 120 unequally spaced burnout states were evaluated.

2.4. Approximation approaches

The presented approach of calculating averaged scattering properties requires a repeated computationally expensive evaluation of the equations resulting from Mie theory. For the application in a numerical simulation of coal combustion, a computationally less expensive calculation procedure is desirable. Therefore, approximate methods are introduced.

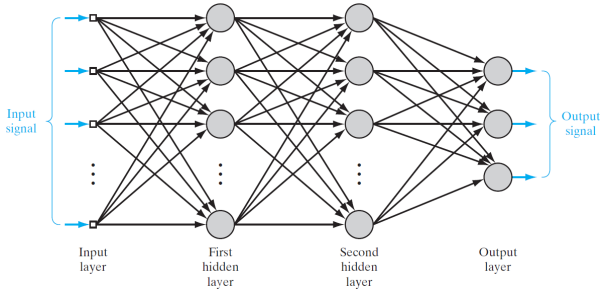


Figure 2: Architectural graph of a multilayer perceptron with two hidden layers. A detailed depiction of a single neuron is shown in Fig. 3 (Source: [1])

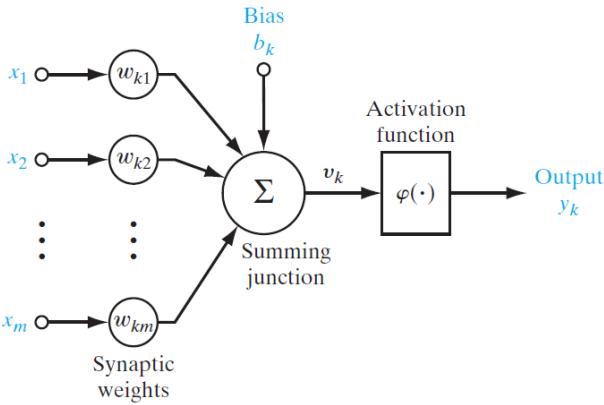


Figure 3: Sketch of the connections to k th neuron in a neural network (Source: [1])

Several approximate phase functions are available, (see e.g. [10]), but their usefulness for application in coal combustion is limited [7]. In the authors' previous studies, a tabulation technique was investigated [10]. In the present study, the suitability of artificial neural networks for the approximation of scattering properties is investigated.

2.5. Artificial Neural Networks

In principle, artificial neural networks can be applied to perform many tasks, such as pattern recognition or classification problems [1]. In the present investigation, their capability for function approximation and interpolation is used.

In this study, a feedforward multilayer perceptron (MLP) has been applied. The architecture of an MLP is displayed in Fig. 2. An MLP consists of an input layer, an output layer and one or more hidden layers. Each hidden layer contains a number of neuron elements that are connected via synapses to the neurons of the next layer. These synapses are weighted by synaptic weights w to strengthen or weaken the connection between two neurons (see Fig. 3 for an illustration). The information incoming into each neuron is summed up and a bias b is applied. An activation function is applied to compute the output y .

Usually, sigmoid functions are chosen as a transfer function, since they are bounded, continuous, differentiable and monotonically increasing. Differentiability is a necessary condition to perform training by backpropagation of errors in

Table 1: Parameter set for averaged scattering and absorption properties

Parameter	Symb.	Value
Planck Temperature, K	T	1700
Mean Diameter for coal, μm	D_m	100
Mean Diameter for ash, μm	D_m	10
Spread of PSD	n	3.5
Refractive index of coal	m_c	see Fig. 1
Refractive index of ash	m_a	see Fig. 1
Spectral range, μm	λ	0.3–12
Diameter Range, μm	D_m	8–120
Discrete burnout states	n_B	120
Discrete scattering angles	n_θ	40000

the training of the network. Thus, in the present investigation, the sigmoid function hyperbolic tangent was applied for the hidden layers, the input and output layers made use of a linear transfer function. The size of the hidden layer can be chosen freely, the size of the input and the output layer is equal to the size of the input and output data for each data-point respectively.

For the present investigation, the input values consist of the burnout B and the scattering angle θ . From these inputs, the value for a specific scattering angle is calculated by the network. The efficiencies, a vector consisting of two entries, can be computed by a separate net, requiring only the burnout as an input.

The training of the network was performed by backpropagation of errors with the Levenberg-Marquardt algorithm [1]. Thereby, the synaptic weights and the bias are adjusted, so that the output of the network matches the training data. The implementation provided by the framework of MATLAB was applied. The training data was generated using equations resulting from Mie theory.

Note that a neural network can suffer from overfitting, an effect that occurs when the network is very large or complex with regard to the data available. To avoid overfitting, all networks that were investigated are small with regard to the training data set consisting of 120 values for B and 40000 values for θ , which results in 4.8 million single training data-points for the phase function Φ .

To represent a neural network, the following notation was chosen: $[n_1 n_2 \dots n_i]$ with n_i representing the number of neurons in the hidden layer number i .

2.6. Investigated Case

In the present investigation, a specific set of parameters determining the scattering behavior was investigated, see Table 1. Considering their influence on the phase function and efficiencies, the most important parameters are the mean diameters and the refractive indices of coal and ash respectively.

3. Results and Discussion

3.1. Averaged Scattering phase function and Efficiencies

Averaged scattering properties are computed as described in the methods section. The result for the phase

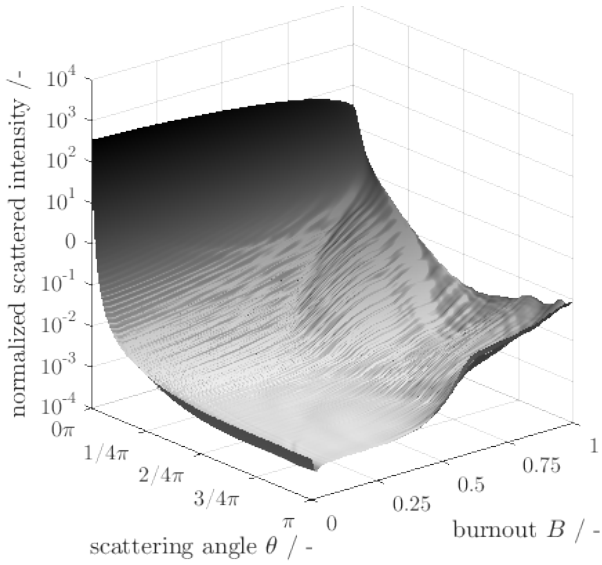


Figure 4: Surface plot of normalized intensity over scattering angle and burnout progress. Intensity is normalized to yield a value of 1 for the sum over θ for each burnout state B

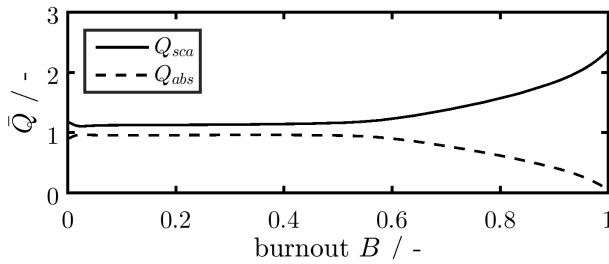


Figure 5: Scattering and absorption efficiencies over burnout

function Φ depending on scattering angle θ and burnout B is shown in Fig. 4.

The efficiencies depending on the burnout state of the particles are presented in Fig. 5. Graphs for the case of coal and ash as well as selected intermediate states are shown in Fig. 6.

The surface plot of the scattering phase function over Φ and burnout in Fig. 4 gives insight on the scattering behavior during burnout. A shift from close to purely forward scattering for coal ($B = 0$) to a more pronounced scattering behavior in different directions than forward, including a stronger amount of backscattering can be observed for values of B larger than $B = 0.5$. A strong ripple structure is found, that is due to the interferences occurring when light is scattered by a particle. Surprisingly, these ripples are not flattened out by the averaging procedure introduced in the methods section, but are still visible in logarithmic scale.

3.2. Approximation Quality and Optimized Network Architecture

The architecture of an artificial neural network has to be chosen so that size and functionality are balanced well for the task at hand and overfitting can be prevented [1]. To determine such an architecture, several different designs and

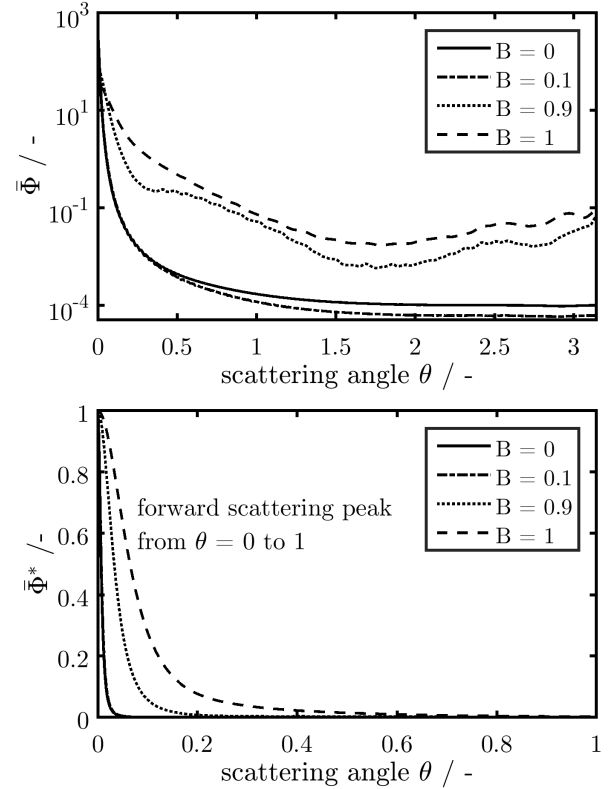


Figure 6: Upper plot: scattering phase function for selected burnout states, log scale. Lower plot: forward scattering peak, normal scale, θ ranges from 0 to 1. Note that the plots are normalized to yield 1 for $\theta = 0$ for comparison

thereby sizes are compared to yield an optimal function approximation ability in this study. The phase functions calculated with selected networks are presented in Fig. 7.

Networks with a large number of hidden neurons are expected to capture the phase function more accurately, whereas small networks require less disk space. However, large networks are more likely to suffer from overfitting. In general, all artificial networks applied here are capable of capturing the profile of the phase function for all burnout states. Nevertheless, differences in approximation quality depending on the type of network can be observed. The network with the architecture [10 15 10] (number of neurons in each hidden layer) follows the general trends of the given phase function very well and can also follow the small oscillations occurring for $B = 0.75$ and $B = 1$.

The network with the architecture [5 9 5] shows difficulties with approximating the oscillations correctly, although the general trends are met. The network with the architecture [5 3] gives only a rough representation of the phase function. The network is probably too small to be able to reproduce the complex shape of the original data.

The major advantage of a neural network compared with conventional methods, e.g. analytical phase functions, is the ability to approximate unknown functional correlations. For an analytical approximation, such a correlation has to be carefully selected for each case specifically. A neural net-

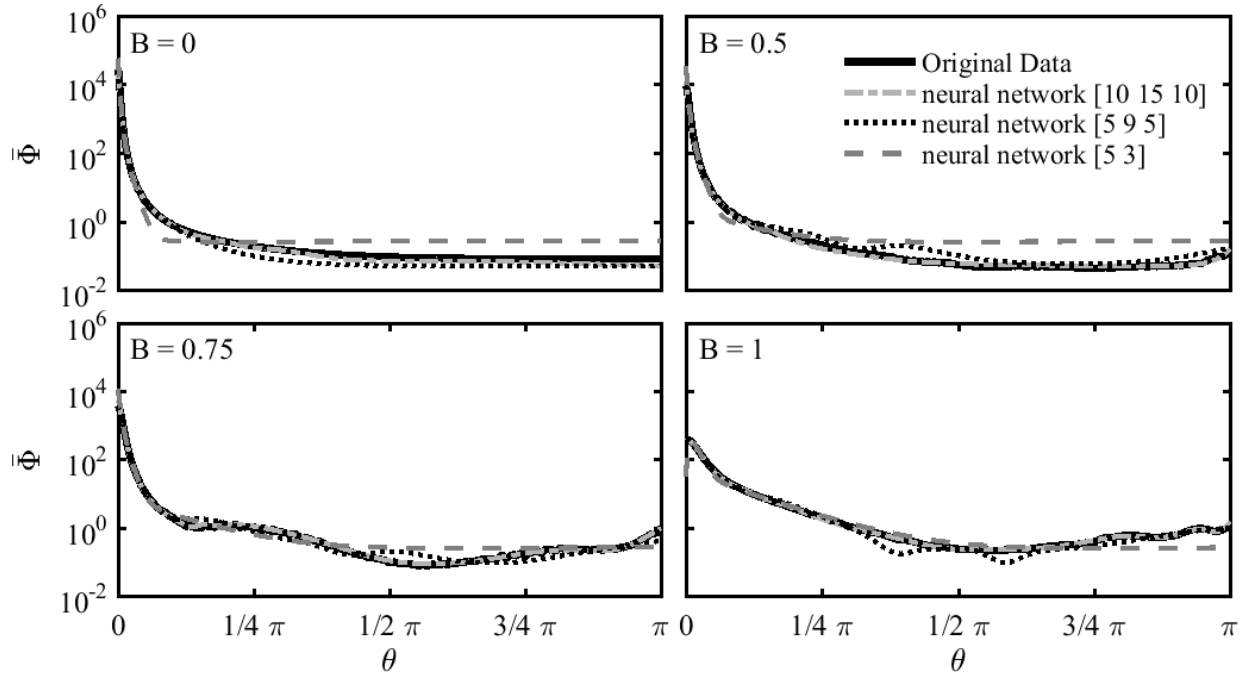


Figure 7: Approximation with artificial neural networks for different burnout states

 Table 2: Tested artificial neural networks (excerpt) and relative deviation to Mie theory (averaged over relative deviation for each scattering angle Φ and burnout state B)

Network architecture	Relative deviation
[10 15 10]	0.0664
[10 15]	0.0719
[10 15]	0.1486
[5 9]	0.1884
[5 9]	0.1914
[5 9 5]	0.1958
[5 9]	0.1987
[5 9]	0.3440
[5 9]	0.4013
[5 10]	0.7705
[4 6]	0.9665
[5 3]	1.3637
[20 10]	12.0843
[2 3]	12.0970
[3 6]	33.1342
[15 10 5]	36.5046

 Table 3: Tested artificial neural networks (excerpt) and relative deviation to Mie theory for scattering and absorption efficiencies (averaged over relative errors for each burnout state B)

Network architecture	Q_{abs}	Q_{sca}
[5 7]	1.80e-04	2.74e-04
[5 10]	1.88e-04	0.00190
[5 9]	2.02e-04	2.25e-04
[7 3]	3.07e-04	7.55e-04
[5 5]	3.09e-04	2.03e-04
[5 6]	3.46e-04	0.001
[7 9]	4.86e-04	0.00210
[10 10]	0.0011	9.15e-04
[20 10]	0.00115	0.00150
[5]	0.0016	0.0012
[5 7 9]	0.0021	8.16e-04
[10]	0.0023	4.36e-04
[7 7]	0.0037	2.99e-04
[3]	0.0055	0.002
[1]	0.0494	0.0114

work is able to identify the structure of a function in training and store it within its neurons and synapses and thereby avoid the effort required to find a suitable analytical function. The advantage of a neural network over table interpolation from previously stored data lies in its significantly lower memory requirement.

The size of the network is an important factor that influences the ability of the network to approximate functions (see Table 2). But the architecture in terms of the numbers of neurons per layer and numbers of hidden layers can also influence the approximation quality.

However, deriving rules to identify an architecture with good approximation quality is not straight forward. Several very different network architectures show reasonable approximation qualities. Other network designs with architec-

tures similar to those with very good approximation quality show poor results (see Table 2). Therefore, one of the main difficulties in the application of artificial neural networks is to choose an appropriate network design. Also, training the network with a different subset of the training data may lead to slightly different results.

A comparison of the approximation quality for the scattering and absorption efficiencies with different network architectures is shown in Table 3. All networks showed very good approximation quality, even a network with just one neuron was able to represent the scattering and absorption efficiencies with a relative deviation of 0.0494 and 0.0114 respectively.

3.3. Memory requirement and speed of evaluation

Ihme et al. [2] found that the evaluation time for an ANN is approximately 5 times higher than an efficiently implemented data storage and retrieval technique. In the present study, this observation has been confirmed.

The storage requirement for the networks applied is below 10 kB for the largest network presented here. Note that the Matlab ANNs can serve for a variety of purposes and therefore may provide features (e.g. adaption) not applied here. Several variables of the datatype string are stored with the network, denoting the activated functions. Therefore, an efficient implementation optimized for memory reduction might reduce this requirement significantly. The number of weights stored for the largest network is 366.

The storage requirements for matrices containing the data required for table interpolation are significantly larger. A very small table, consisting of values for 25 burnout states and 400 scattering angles already requires 72 kB of memory, storing 10000 data points. The matrix containing 50 burnout states and 4000 scattering angles requires a size of 1.5 MB, the matrix applied in the training of the ANNs with 120 burnout states and 40000 scattering angles requires 7.7 MB.

This matrix only includes the data computed for the parameters listed in Table 1. If scattering phase functions for a broader range of parameters have to be stored, these memory requirements increase, therefore the application of models is inevitable. A promising option is provided by artificial neural networks.

4. Conclusions

In the present paper, the representation of the scattering phase function (and scattering/absorption efficiencies) was discussed. The approximation with artificial neural networks yielded a very good approximation quality for specific network designs. The identification of these designs is not straightforward. Additionally, the training of such an artificial neural network is time consuming and requires experience, since training can fail and the approximation quality can vary for network architectures that are similar at first glance.

However, the results presented here show that artificial neural networks can be successfully applied to approximate complex scattering phase functions in particle radiation interaction in numerical simulations of pulverized coal combustion.

Acknowledgements

This work has been financed by the German Research Foundation (DFG) within the framework of the SFB/Transregio 129 “Oxyflame”.

The Authors also thank Justus Zinn for his contributions to this work.

References

- [1] S. Haykin, Neural networks and learning machines, Pearson, New York, 1999.
- [2] M. Ihme, C. Schmitt, H. Pitsch, Optimal artificial neural networks and tabulation methods for chemistry representation in les of a bluff-body swirl-stabilized flame, Proceedings of the Combustion Institute 32 (2009) 1527–1535.
- [3] G. Mie, Beiträge zur Optik trüber Medien, speziell kolloidaler Metallösungen, Annalen der Physik 330 (3) (1908) 377–445.
- [4] C. F. Bohren, D. R. Huffman, Absorption and scattering of light by small particles, Wiley, New York, 1983.
- [5] O. Pena, U. Pal, Scattering of electromagnetic radiation by a multi-layered sphere, Computer Physics Communications 180 (11) (2009) 2348 – 2354.
- [6] W. Yang, Improved recursive algorithm for light scattering by a multi-layered sphere, Applied optics 42 (9) (2003) 1710–1720.
- [7] M. F. Modest, Radiative Heat Transfer, 3rd Edition, Academic Press, 2013.
- [8] S. Manickavasagam, M. P. Mengüç, Effective optical properties of pulverized coal particles determined from ft-ir spectrometer experiments, Energy & Fuels 7 (1993) 860–869.
- [9] M. Neubronner, Strahlungswärmeübertragung von Aschepartikeln aus Kohlefeuerungen, Ph.D. thesis, TU München, Germany (1995).
- [10] T. Gronarz, O. Hatzfeld, M. Habermehl, R. Kneer, On the Importance of Particle Radiation Interaction in the Numerical Simulation of Pulverized Coal Combustion, in: 10th European Conference on Industrial Furnaces and Boilers: INFUB 10, 02.07.2015 - 02.10.2015, Porto, Portugal, 2015.

Nomenclature

θ	Scattering angle, -
φ	Activation function, -
B	Burnout progress, -
C	Crosssection, μm
E	Planck spectral intensity distribution, -
n_{RR}	Spread parameter (Rosin Rammler PSD)
P	Particle size distribution, -
Q_{abs}	Absorption efficiency, -
Q_{sca}	Scattering efficiency, -
w	Synaptic weights, -
x	Dimensionless size parameter $x = \frac{\pi D}{\lambda}$, -